BNL-76727-2006-CP

Instabilities in NB_3SN Wires

Lance Cooley and Arup Ghosh

June 2006

Condensed Matter Physics and Materials Sciences Division

Brookhaven National Laboratory
P.O. Box 5000
Upton, NY 11973-5000
www.bnl.gov

Notice: This manuscript has been authored by employees of Brookhaven Science Associates, LLC under Contract No. DE-AC02-98CH10886 with the U.S. Department of Energy. The publisher by accepting the manuscript for publication acknowledges that the United States Government retains a non-exclusive, paid-up, irrevocable, world-wide license to publish or reproduce the published form of this manuscript, or allow others to do so, for United States Government purposes.

DISCLAIMER

This report was prepared as an account of work sponsored by an agency of the United States Government. Neither the United States Government nor any agency thereof, nor any of their employees, nor any of their contractors, subcontractors, or their employees, makes any warranty, express or implied, or assumes any legal liability or responsibility for the accuracy, completeness, or any third party's use or the results of such use of any information, apparatus, product, or process disclosed, or represents that its use would not infringe privately owned rights. Reference herein to any specific commercial product, process, or service by trade name, trademark, manufacturer, or otherwise, does not necessarily constitute or imply its endorsement, recommendation, or favoring by the United States Government or any agency thereof or its contractors or subcontractors. The views and opinions of authors expressed herein do not necessarily state or reflect those of the United States Government or any agency thereof.

Printed on recycled paper

BNL-76727-2006-CP

INSTABILITIES IN NB_3SN WIRES

Lance Cooley and Arup Ghosh
Brookhaven National Laboratory, Upton NY 11973 USA

Abstract
High current-density Nb_3Sn strands made by internal-tin routes are not stable against flux jumps at low fields. Since flux jumps release heat, they can initiate quenching if thermal conductivity to the liquid helium is poor. To make matters worse, tin is a potent contaminant of copper, and reaction of strands to maximize performance leads to the loss of thermal conductivity. We discuss how the root of a solution of this problem lies in optimizing two parameters, *RRR* and J_c, instead of J_c alone. An important workaround for magnet designers is controlling the balance between performance and stability by reducing the temperature or time of the final heat treatment step. This provides ample J_c while also keeping *RRR* high. Under these conditions, the instability current density threshold J_s is higher than J_c. Additional factors are also available to improve the management of instabilities, including new strand designs with smaller subelements or divided subelements.

INTRODUCTION

We review recent work to understand and overcome instabilities in high-J_c Nb_3Sn strands developed for high-field dipole and quadrupole magnets. A general specification by magnet programs is for strands to have very high critical current density J_c, such as the 3,000 A mm^{-2} target of the U.S. HEP R&D program. This presents two central problems to the operation of a stable magnet. First, the tendency to maximize critical current density leads to consolidation of filaments into a single mass and substantial reaction of the Nb diffusion barrier, creating an effective diameter that is equal to the diameter of the subelement itself. Second, the tendency to react substantial fractions of the diffusion barrier brings the tin perilously close to or in contact with the copper stabilizer, resulting in contamination of the copper and loss of its electrical and thermal conductivity. In combination, these problems can prevent the operation of an accelerator magnet because flux jumps initiate quenches in the low-field portions of the magnet.

There are several strategies to work around these problems, which we outline in this report. Foremost is the implementation of less aggressive reaction heat treatments, which preserve the stabilizer and, rather remarkably, produce current densities almost as high as the maximum that can be obtained. In addition, we discuss progress in other strategies, including subdividing the subelement to reduce the effective diameter of the superconductor, increasing the number of subelements to reduce their diameter at given wire diameter, and varying the ratio of subelement perimeter to its area. We also discuss measurements and diagnoses.

KEY FEATURES OF MODERN ACCELERATOR MAGNET STRANDS

Almost all internal-tin wire designs now being used greatly restrict the amount of interfilamentary copper to maximize the subelement fraction that is converted to superconductor after reaction. This increases the non-copper J_c. As a result, filaments merge into a solid mass during the reaction heat treatment, producing a large characteristic size over which magnetization and transport currents flow (the effective diameter).

In addition, wire manufacturers have found it beneficial to wrap each subelement restack with its own diffusion barrier, instead of using a single diffusion barrier around the entire filament pack (as is used in many wires for the International Thermonuclear Experimental Reactor). A significant fraction of the diffusion barrier is subsequently reacted; this is *intended* in the design of most strands. Since the diffusion barrier forms an annulus around (and often merged with) the filament pack, its partial reaction alone can produce a large effective diameter. Even if the filaments are tightly packed, the modern reaction prescriptions are quite successful at distributing tin throughout the subelement during the low-temperature steps of the reaction, and it is difficult to avoid any reaction of diffusion barriers made from Nb. Other barrier materials, such as Ta and V, are not as ductile and can be prone to thinning or even rupture.

As pointed out by Wilson [1], an adiabatic stability threshold is crossed when the magnetic energy stored within the critical state exceeds the heat capacity of the superconductor and its thermally bonded copper. Given that subelement diameter $d_s = d_w\ [N(1+R)]^{-0.5}$, where N is the number of subelements and R is the stabilizer to non-stabilizer area ratio, typical values of d_s are ~100 μm for wire diameters d_w of approximately 1 mm. For a 100 μm subelement carrying a current density of 3,000 A mm^{-2} at 12 T and 4.2 K, the heat capacity of a strand (~1,000 J m^{-3} K^{-1}) and its ~15 K operating margin barely meet this stability criterion against small disturbances. This means that flux-jump instabilities are essentially inevitable at low fields, due to the faster-than-linear increase of J_c with decreasing field. So far, all internal-tin strand designs exhibit flux jumps at low fields.

Since flux jumps deposit heat into a magnet, management of the heat is an important task to ensure safe operation. Here, however, the potency of tin for scattering electrons in copper is an obstacle. According to Fickett [2], even as little as 0.1% Sn (atomic %) is sufficient to reduce the residual resistivity ratio RRR of copper to 7. This contamination level is well below that which can be reliably detected by micro-chemical analyses, which are sensitive to 0.5%. Any drop in RRR from its value of ~300 for oxygen free high-conductivity copper signals significant contamination. For example, if two parallel copper pathways are considered, one with RRR = 266 and the other with RRR = 7, fig. 1 shows that a significant fraction the total electrical pathway must consist of the contaminated portion by the time a decrease of RRR to ~100 occurs.

Reaction heat treatments often produce the maximum J_c value by maximizing the area fraction of the subelement that is converted to Nb_3Sn. Since Nb diffusion barriers have the best ductility and produce the most uniform subelements, this means that partial reaction of the barrier is intended, bringing the tin supply close to and then in contact with the copper stabilizer. Thus, maximum J_c is correlated with tin reaching the copper and a reduction of RRR. So, while magnet R&D programs have emphasized maximizing J_c to provide headroom for solving other problems, they also facilitate loss of electrical and thermal conductivity of the copper matrix. This reduces both heat conduction to the liquid helium bath and inductive coupling to retard the flux jump. The specific behavior, which obeys complicated sets of coupled nonlinear thermo-electromagnetic equations [3], are beyond the focus of our review. What is essential is that the two problems above can combine to initiate quenches in the low-field portions of magnets.

STABILITY CURRENT DENSITY

During the past 4 years, new test mandrels and new testing procedures have reduced the tendency for Nb_3Sn strands to quench during standard critical current measurements. Key improvements include control of strand motion, support for transport current across transition zones, and lengthening of the current input region. These improvements now make it routine to attain stable voltage vs. current curves (*V-I* plot) at fields above about 8 tesla, where critical currents can approach 1,000 amperes, which allow the extrapolation of a critical current criterion through the measured data. Below this field range, quenches of the strand often occur well below the critical current. Flux jumps can be triggers for these quenches. Significant efforts at Fermilab and at Berkeley have mapped out in detail

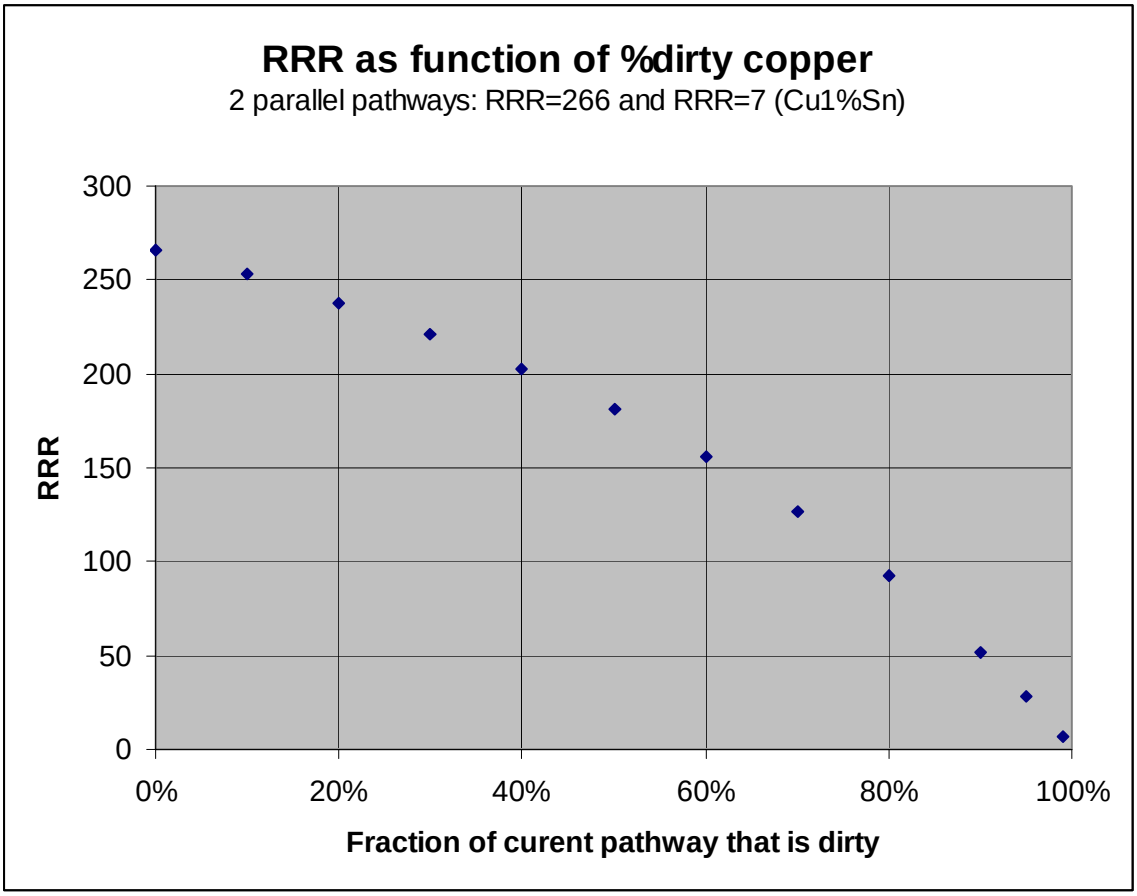

Fig. 1. *RRR* calculated for a bimetal composite strip, consisting of a fraction *f* of "dirty" copper (RRR = 7, resistivity at room temperature = 1.88 μΩ cm) and a remainder (1-*f*) of "clean" copper (RRR = 266, resistivity at room temperature = 1.00 μΩ cm), as a function of the fraction of "dirty" copper.

the quench thresholds for various regimes of field, strand diameter, subelement number, and so on, and the observed boundaries appear to be consistent with stability calculation.

However, the multiple potential quench triggers in a short-sample experiment, let alone in a magnet, make it difficult to decipher whether in fact flux jumps initiate quenching or whether other sources, such as mechanical motion, become active as the testing current increases. This distinction is important, because flux-jump instabilities are intrinsic to the properties of the strand itself, whereas other triggers are related to the quality of test fixture or magnet assembly. Magnetization measurements, in which the sample is free from mechanical binding, definitely show that all internal-tin strands used in HEP programs experience flux jumps at low fields. Here, the magnetic moment of the sample is monitored while the magnetic field is swept with the sample held at constant temperature. Since vapor cooling is typically used in magnetometers, these experiments are conducted at a lower stability than for samples immersed in a coolant bath.

Our recent work [4,5,6] outlines an experimental technique to determine the maximum current density that can be passed through a strand experiencing a flux jump and still able to recover. Like magnetization experiments, the sample is held at constant temperature under a field sweep. However, this is conducted while the sample also carries a constant transport current and while it is immersed in the liquid helium bath. The transport current is at or below the current used to generate successful a *V-I* plot at higher fields, making other triggers of flux jumps unlikely. The resulting plot of voltage versus field (*V-H* plot), such as that in fig. 2, typically shows numerous voltage spikes, which are generated by flux jumps as the current and field profiles inside the strand alter to accommodate the

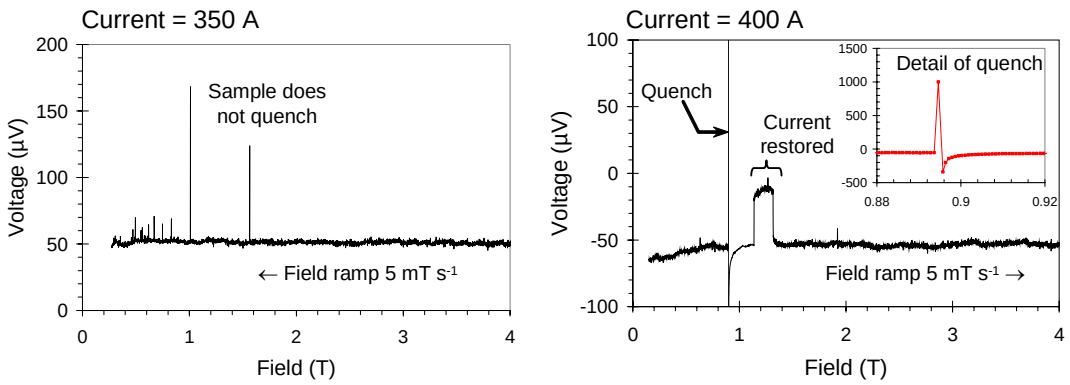

Figure 2. *V-H* plots for two different settings of constant applied current. At left, a current of 350 A is below the threshold where the heat released by flux jumps causes the strand to quench. At right, a higher current, 400 A, produces a quench that drives the conductor above the critical temperature, tripping detection circuitry on the power supply.

external field change. Since the strand J_c can be very high in this field range (0 to 4 tesla), the critical current lies far above the transport current, and there is ample capacity to accommodate current transfer between the subelements. It is also important to recall that even though the transport current can be carried by a small fraction of the total number of subelements at low field, all subelements are fully carrying induced magnetization currents if the field has been ramped over an interval larger than the penetration field, typically < 1 T. The central question, then, is whether the thermal perturbations caused by the current and flux rearrangements can escape to the coolant bath without quenching the strand.

After measuring a number of *V-H* curves at different applied currents, it is typically seen that the applied current is correlated with the likelihood that a flux jump will quench the strand. This correlation allows a stability current density threshold, J_s, to be defined by the maximum current at which flux jumps do not result in quenching of the strand. In fig. 2, this threshold current is between 350 and 400 A, yielding J_s of ~1400 A mm^{-2} for this 0.8 mm diameter strand (50% copper stabilizer).

BALANCING J_C, J_S, AND *RRR*

As mentioned earlier, a nearly complete reaction of the diffusion barrier is intended in most internal-tin strand designs, following from a strategy of maximizing superconductor area while just avoiding tin contamination. However, since Nb_3Sn wire fabrication is complex, it is very difficult to design a barrier thickness that is just enough to ensure reaction of all of the Nb filaments while also avoiding tin contamination for a given reaction sequence. Instead, the optimum heat treatment matrix is determined empirically.

Reducing the time or temperature of the reaction reduces the amount of filament and barrier area that is converted to Nb_3Sn, effectively trading performance to better ensure copper purity. A key question, then, is to what extent is J_c reduced by limiting the final reaction duration? Before about 2003, work on modified jelly-roll strand designs indicated that the falloff could be quite large, perhaps 30%. A second question is whether the stability current density is correlated with *RRR* at all.

In 2004, we conducted experiments to probe explicitly these questions. Fig. 3 summarizes the results, as published recently in [4]. The strands used for this experiment are 54-subelement restacked-rod process (RRP) wires from Oxford Instruments – Superconducting Technology (OI-ST), which are the progenitors of the present LARP strand design. First, as final reaction duration increases, there is a steep falloff of *RRR*, indicating that there is substantial diffusion of tin into the copper even after 24 hours. For reference, final reaction times for modified jelly-roll wires could be as

long as 200 hours. Second, there is a strong correlation between J_s and *RRR*, indicating that the loss of thermal conductivity indeed causes a reduction in the strand's ability to survive flux-jump instabilities. Third, there is very little variation of J_c with reaction time, where 90% of the maximum J_c is reached already at only 24 hours. Fourth, and most importantly, J_s falls below J_c when the final reaction step exceeds about 45 hours. This indicates the crossover for operation of a magnet, because the load-line passes through an instability region at low fields. In other words, flux jumps in the low-field portions of the magnet will produce quenches when $J_s < J_c$.

While for this particular strand the onset of unstable magnet operation appears to occur for *RRR* of ~20, this value should not be used as a guideline. Instead, the moral of this experiment is that modern strands are provided with tin activity that is so high as to permit short reactions and high *RRR* values without sacrificing performance too greatly. Moreover, since the duration and temperature of the reaction heat treatment are parameters controlled by the magnet designer, the inter-relationship of J_c, J_s, and *RRR* provide the means to adjust the stability of the magnet at the laboratory. For the experiment described in Fig. 3, the extra work in preparation of additional strands, testing, and the implementation of *V-H* plots as a standard characterization tool provided a much more complete knowledge base for magnet construction.

OTHER PARAMETERS THAT MAY AFFECT THE BALANCE BETWEEN PERFORMANCE AND STABILITY

Perimeter-to-area ratio

The RRP conductor design uses barriers around each subelement, often called the distributed barrier approach. In this design, a copper thermal pathway lies next to each potential heat source, connecting it with the coolant bath provided the copper stays clean. This makes the purity of the inter-subelement copper extremely important. When tin contaminates the thin copper regions between subelements, the direct thermal link is broken. Heat generated in an interior subelement must diffuse through neighboring subelements instead, greatly reducing the strand's ability to shed heat and recover. Thus,

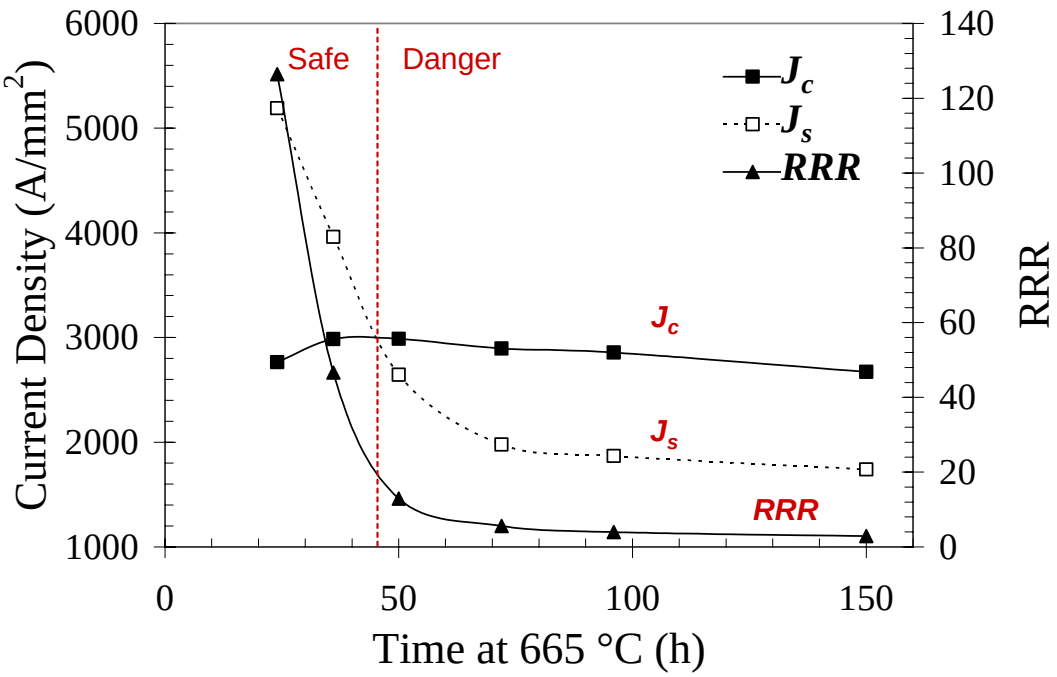

Figure 3. Summary of experiments to determine the optimum balance between performance and stability. The *x*-axis indicates the duration of the final stage of the strand reaction. For times longer than ~45 hours, the stability current density J_s falls below the critical current density J_c, indicating a regime where recovery from flux jumps may not be possible.

tin contamination changes the effective ratio of thermal transfer perimeter to heat generating area from one determined by the dimensions of the subelement to one determined by the dimensions of the strand. That is, the thermal transfer coefficient becomes worse by a factor of approximately $N^{1/2} \sim 7$. This may explain why J_s falls so quickly with reduction of *RRR*.

To explore this hypothesis further, we measured *V-H* data for a high current-density strand design with a single barrier surrounding all of the subelements. The strand chosen was an Outokumpu Advanced Superconductors (OKAS) design with 19 subelements and a Ta diffusion barrier. Despite having *RRR* of 235, *V-H* data showed that J_s was only 566 A mm^{-2}. This is only 2/3 the J_s of an RRP strand with *RRR* of only 7 in fig. 3. Although the subelements are larger in the OKAS strand than in the RRP strand, and therefore the heat released by flux jumps is higher than in the RRP strand, the huge difference in J_s clearly points to the significant roles played by the higher perimeter-to-area ratio and the presence of clean inter-subelement copper in the RRP designs.

Subelement diameter and division

An interesting question is whether it is possible to produce subelements that are inherently stable against flux jumps. At the very least, strands that are closer to this stability limit should exhibit better tolerance of tin contamination, due to the smaller amount of heat released by a flux jump. To explore this goal, and to move closer to the DOE-HEP target of 40 μm subelement diameter, OI-ST has produced RRP conductors with up to 216 subelements. As discussed earlier, the subelement diameter scales with $N^{-1/2}$ for constant copper fraction (which is usually close to 50% of the strand area). For a 0.8 mm strand and 50% copper fraction, $N = 216$ yields a subelement diameter of 38 μm.

However, the ductility of strands with high subelement number is not as good as for lower subelement number. The materials science beneath this observation is just in its early stages of study. Nonetheless, the difficulties in strand drawability produce two important consequences for stability. First, distortions of the subelement shape produce regions where the diffusion barrier is thin, exacerbating the potential for tin contamination of the copper. In fact, our examinations showed a reduction of *RRR* despite no visible points of tin break-through by scanning electron microscopy for a 126-subelement design, suggesting that controlling tin contamination is even more subtle. Second, distortions of the subelement shape also increase the dimension over which magnetization currents flow, adding to the magnetization. Figure 4 shows how these distortions produce effective filament diameters that are larger than the calculated diameter for a round subelement.

Significant improvement has come from strategies to divide the ring of filaments that make up the subelement. OI-ST described processes for inserting foils or spacers in published work. As seen in fig. 4, this approach is much more successful at reducing the effective filament diameter than increasing the subelement diameter has been. The drawback is the reduction in superconductor area, since about 10% of the subelement area (and sometimes more) is taken up by the dividers.

Estimating RRR

Measurements of *RRR* can be routinely done as part of other testing. For instance, at BNL we record the sample resistance as the helium boils away overnight following a series of testing experiments. A new probe has been set up to measure multiple samples simultaneously. However, the opportunity for making *RRR* measurements, especially the availability of liquid helium, need not revolve around the schedule of the test facility. After comparing ~50 different samples with a wide range of *RRR*, we

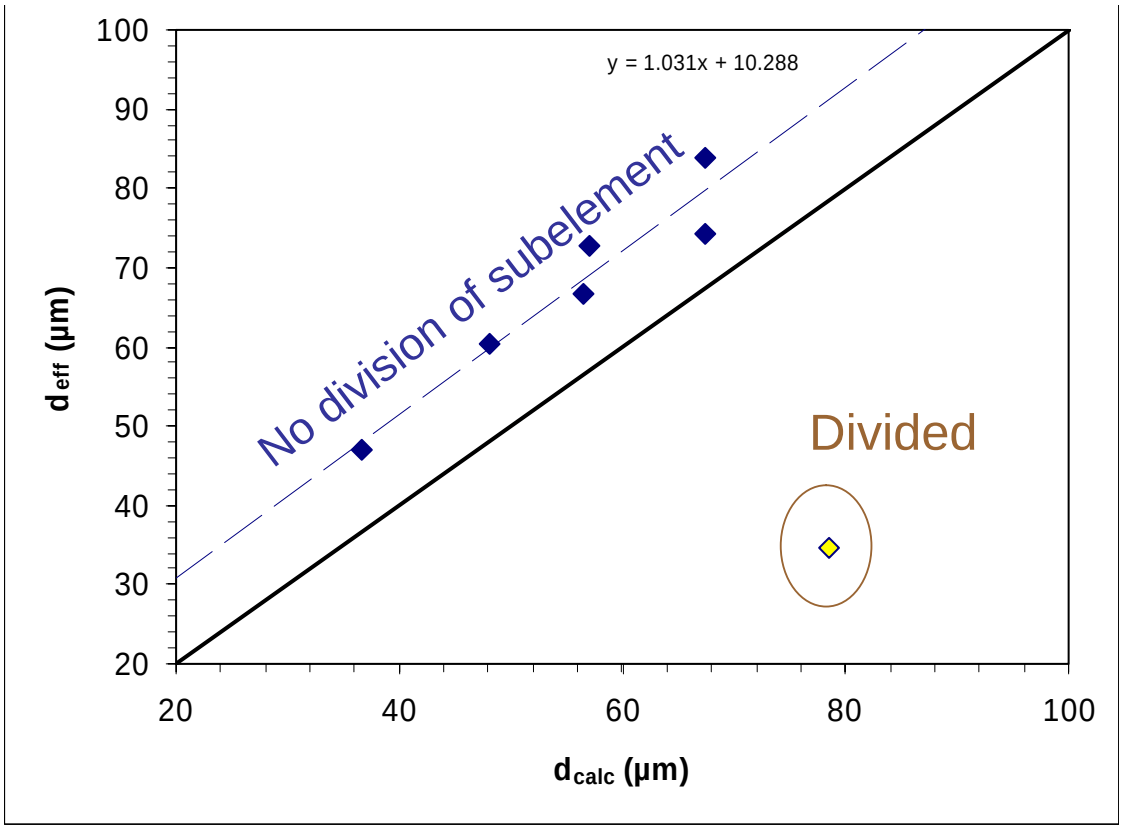

Figure 4. Effective filament diameter (determined from magnetization and extrapolated transport measurements) plotted against the calculated subelement diameter (determined by wire diameter, subelement number, and copper fraction). The black line denotes $d_{eff} = d_{calc}$. Increasing the number of subelements produces data with a comparable slope (dashed blue line) but offset due to distortion of the subelement shape. Division of the subelement is more effective, but with a performance penalty.

observed a strong correlation between *RRR* and the value of residual resistance determined at liquid nitrogen temperature (*Rr* = resistance at 300 K divided by the resistance at 77 K):

$$RRR = 0.47 \exp(0.81\, Rr).$$

The quality of this estimation is shown in fig. 5 for a number of RRP strands.

Effects of reaction temperature

Besides limiting the duration of the final reaction stage to preserve high *RRR*, it is possible to reduce the reaction temperature for comparable time to achieve the same effect. Based on data for the reaction rates of high-tin bronze composites, the growth rate of the Nb_3Sn layer approximately doubles for every 50 °C increase in temperature near 700 °C. This means that a 24-hour reaction at 695 °C (as specified by the manufacturer) could be lengthened to 48 hours at 650 °C to obtain approximately the same non-copper area of Nb_3Sn. The advantage of longer time at lower temperature is a wider window to detect and control the onset of tin contamination, providing a better ability to optimize both J_c and *RRR*.

We have explored the effects of time and temperature on strand properties over a wide range of reaction parameters using the same RRP wire. These results are summarized in fig. 6 for the LARP strand design (OI-ST billet 8220-4 at 0.7 mm diameter). There are several points to note. First, increasing the reaction temperature generally drives down *RRR* regardless of the reaction duration. Second, there is a rather wide temperature range, at least 50°C, that can be used to obtain J_c close to 3000 A mm^{-2} at 12 T, 4.2 K. Under these circumstances, better combinations of J_c and *RRR* are seen for reactions at 650 °C than at 665 or 680 °C. For these reasons, we now favour the lower reaction temperatures.

SUMMARY

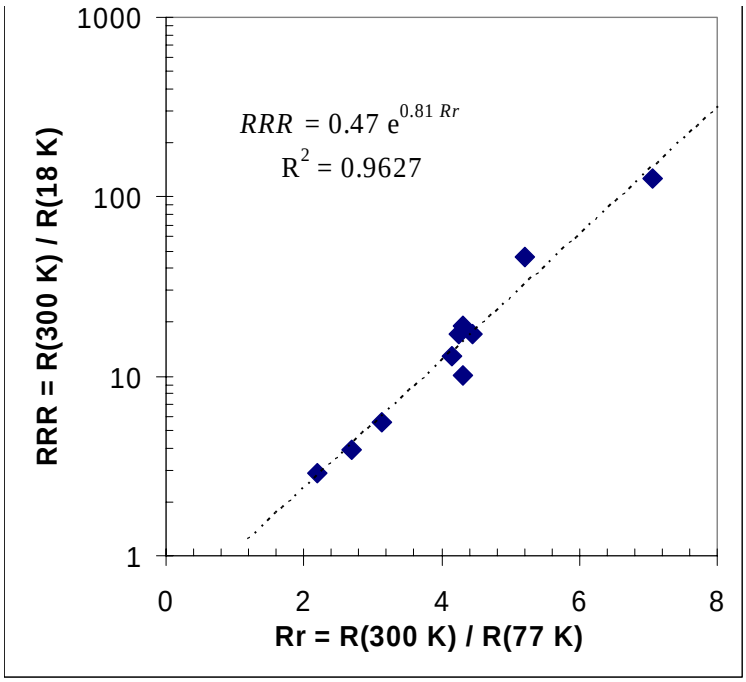

Figure 5. Measured value of *RRR* plotted against the residual resistance determined at liquid nitrogen temperature (*Rr*). The dashed line indicates the fit by *RRR* = 0.47 exp (0.81 *Rr*), which has a high quality of regression as indicated.

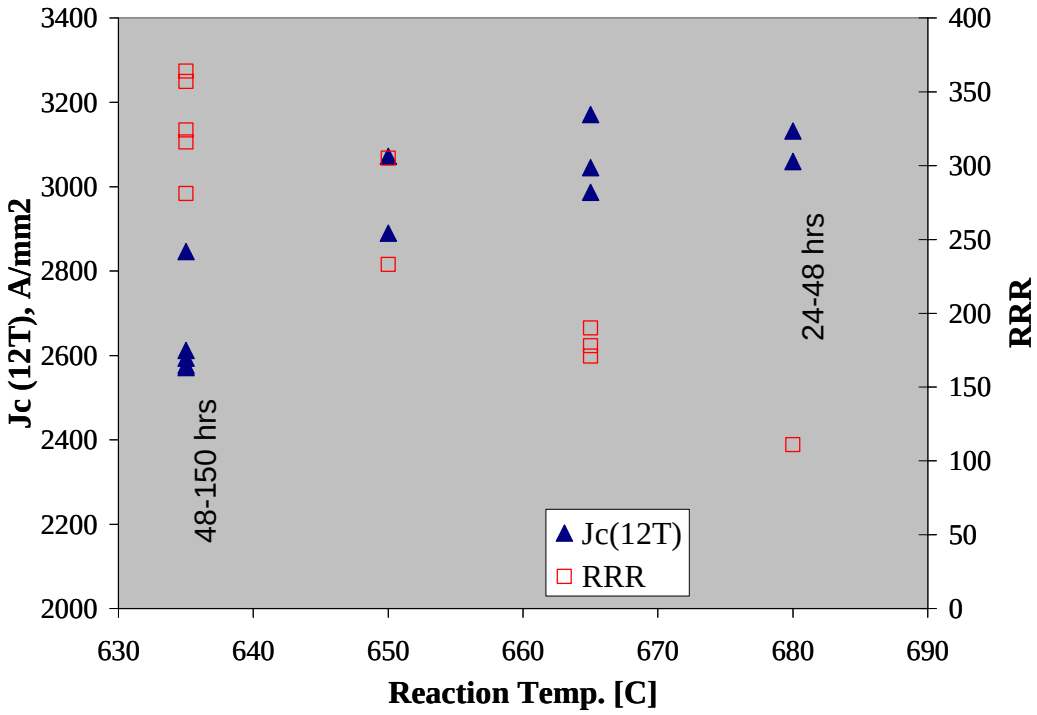

Figure 6. Critical current density and *RRR* as a function of reaction temperature during the final heat treatment stage. Reaction times range from 48 to 150 hours at 635 °C and just 24 and 48 hours at 680 °C. While J_c is optimum for the 665 °C, 72-hour reaction, the 650 °C, 48-hour reaction gives a good combination of high J_c and high *RRR*.

Flux-jump stability problems are difficult to avoid altogether because of metallurgical issues associated with ductility, shape control, piece length, and the design of the Nb_3Sn strands. Since almost all existing Nb_3Sn strands display flux jumps, magnet designers should not overlook the possibility of flux-jumps, and they should take prudent steps to manage the heat released. An important control is the somewhat delicate balance between performance (J_c) and stability (*RRR* and J_S). It was shown that a necessary condition for safe magnet operation is $J_s > J_c$, which is ensured by keeping *RRR* high. Recent strand designs provide for some flexibility in choosing the reaction heat treatment, because J_c reaches high values rather quickly, so the sacrifice in performance to preserve stability is not large.

New characterizations were developed to probe the flux-jump instability. In particular, the *V-H* plot has become a standard measurement in our laboratory. This technique determines the instability current threshold with less ambiguity than current-voltage measurements because it reduces problems associated with current injection into the strand and mechanical motion. Simplification of the measurement of *RRR* by using a liquid-nitrogen measurement was also discussed.

Our experiments also revealed a tendency for reactions at temperatures above 650 °C to degrade *RRR* rather strongly, even for reactions as short as 24 hours in the final stage. A better combination of high *RRR* and good J_c was found for reactions completed at 650 °C. Because the stability-performance balance is a 2-parameter optimization, reactions at lower temperature (650 vs 695 °C) are now preferred for LARP.

REFERENCES

[1] Martin N. Wilson, “Superconducting Magnets”, Oxford University Press 1983.

[2] F. R. Fickett, *Cryogenics* **22**, 135 (1982).

[3] See for instance A. V. Gurevich and R. Mints, Rev. Mod. Phys. **59**, 941 (1987).

[4] A. K. Ghosh, E. A. Sperry, L. D. Cooley, A. R. Moodenbaugh, R. L. Sabatini, and J. L. Wright, *Supercond. Sci. Technol.* **18**, L5 (2005).

[5] A. K. Ghosh, L. D. Cooley, and A. R. Moodenbaugh, *IEEE Trans. Appl. Supercond.* **15**, 3360 (2005).

[6] A. K. Ghosh, L. D. Cooley, A. R. Moodenbaugh, J. A. Parrell, M. B. Field, Y. Zhang, and S. Hong, *IEEE Trans. Appl. Supercond.* **15**, 3494 (2005).